Scripta Materialia 188 (2020) 88–91

Contents lists available at ScienceDirect

Scripta Materialia

journal homepage: www.elsevier.com/locate/scriptamat

Effects of solute oxygen on kinetics of diffusionless isothermal ω transformation in β-titanium alloys

Norihiko L. Okamoto[a], Shuhei Kasatani[a], Martin Luckabauer[a,b], Masakazu Tane[c,d], Tetsu Ichitsubo[a,*]

[a] Institute for Materials Research, Tohoku University, Sendai, Miyagi 980-8577, Japan
[b] Faculty of Engineering Technology, University of Twente, P.O. Box 217, Enschede 7500 AE, the Netherlands
[c] The Institute of Scientific and Industrial Research, Osaka University, Osaka 567-0047, Japan
[d] JST, PRESTO, 4-1-8 Honcho, Kawaguchi, Saitama 332-0012, Japan

ARTICLE INFO

Article history:
Received 13 May 2020
Revised 28 June 2020
Accepted 1 July 2020
Available online 21 July 2020

Keywords:
Titanium alloys
Aging
Differential scanning calorimetry (DSC)
Hardness
Internal friction

ABSTRACT

We have investigated the effects of solute oxygen on the kinetics of diffusionless isothermal omega (DI-ω) transformation in β-titanium vanadium alloys. This transformation constitutes a third category of ω transformation beside the athermal and isothermal modes. Thermal analysis, hardness and internal friction measurements were conducted after quenching oxygen-containing and near-oxygen-free alloys with ~ 21 at%V from the β-stable temperature. At this level of vanadium concentration, the athermal ω transformation is not expected. It is found that the DI-ω transformation more rapidly progresses in the low oxygen alloy and the relaxation strength of the elementary process of $\{111\}_\beta$ collapse is significantly reduced.

Since the omega (ω) phase was first discovered by Frost et al. [1] many researchers have tried to understand the ω transformation mechanism [2–7]. Because the ω phase is brittle and usually undesired for mechanical applications, it is highly desirable to control the kinetics of ω transformation in order to use the alloys in practical applications, exploiting the superior properties of the β phase. From a thermodynamic viewpoint, the ω transformation process has been classified into "athermal" and "isothermal" modes [3,4]. The former takes place via a diffusionless mechanism, whereas the latter is a diffusion-mediated process with a spinodal-like phase separation. In the course of investigation, several researchers have claimed that there exists a peculiar transformation mode that cannot be classified into the conventional two modes [8–10]; a diffuse ω structure, which is an incomplete ω structure also termed "modulated omega" in the de Fontaine paper [3], which can gradually be formed during isothermal aging at around room temperature (RT), although atomic diffusion in the β-titanium alloy systems is hardly possible at such a low temperature.

To clarify these problems, we have recently explored the detailed mechanism of the diffusionless isothermal ω (DI-ω) transformation in the Ti–V alloy system [11]. So far, it is known that the formation of the ω phase tends to be suppressed by solute oxygen and, moreover, the athermal ω transformation temperature, T_ω, is also raised for alloys that contain fewer oxygen atoms [12]. However, there is limited data about the effects of oxygen on the DI-ω transformation. In this work we show how the oxygen atoms affect the DI-ω kinetics and the related changes in mechanical properties such as Vickers hardness and submegahertz internal friction for β-type Ti–V model alloys.

Two types of Ti–V alloy samples with two sets of starting materials were prepared by arc-melting and tilt-casting: (i) 99.9 wt% purity Ti and 99.7 wt% purity V (without regard to oxygen and nitrogen), (ii) 99.999 wt% high purity Ti and 99.7 wt% purity V with an oxygen content lower than 0.1 at%. The final Ti and V contents for the various compositions of Ti–V alloys were determined by inductively coupled plasma-optical emission spectrometry (ICP-OES, IRIS Advantage DUO, Thermo Fisher Scientific Inc., USA) directly after production. The oxygen content in the prepared alloys was determined with an oxygen/nitrogen elemental analyzer (TC-436, LECO Corp., USA) and is plotted in Fig. 1 as a function of V content; the reason why we focus on the V composition is that the former starting material is the main source of oxygen. Three compositions were chosen for the present study: Ti–20.9 at%V, Ti–22.0 at%V (former set), and Ti–21.3 at%V(HP) (the latter using high pu-

* Corresponding author.
E-mail address: tichi@imr.tohoku.ac.jp (T. Ichitsubo).

https://doi.org/10.1016/j.scriptamat.2020.07.005
1359-6462/

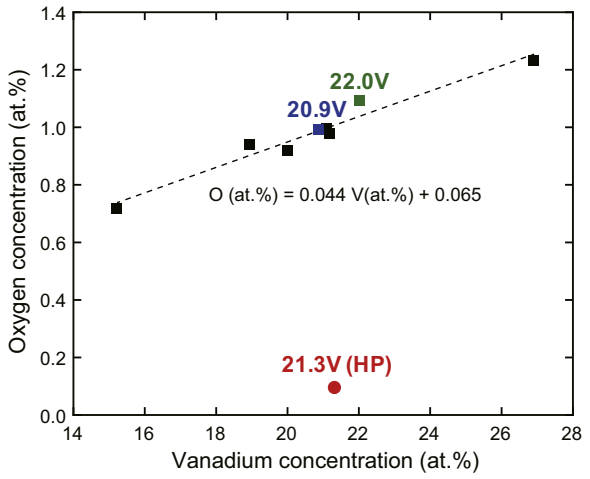

Fig. 1. Oxygen concentration in the prepared Ti–V alloys as a function of V concentration. Most of the samples indicated by (black, blue, green) squares were prepared by using V including a certain amount of oxygen, whereas one sample (marked by red circle) with about 0.1 at% oxygen was prepared using a high purity V starting material. The three samples indicated by blue, green, and red were used in the present study for further analyses. (For interpretation of the references to color in this figure legend, the reader is referred to the web version of this article.)

rity elements). Referring to a previous work [12], T_ω of the respective alloys are estimated to be

T_ω(22.0V) < T_ω(20.9V) ≪ RT for Ti–20.9 at%V and Ti–22.0 at%V, which both include about 1 at%O, and

T_ω(21.3V-HP) ~ RT for Ti–21.3 at%V(HP), which includes 0.1 at%O; RT refers to room temperature. Prior to all measurements, the samples were subjected to solid-solution treatment at 1073 K for 2 h in a vacuum atmosphere at 10^{-3} Pa, followed by quenching in ice water. All the measurements were conducted soon after (within 12 h) quenching the samples to avoid RT aging effects.

To investigate the oxygen effects on the DI-ω transformation kinetics, we compare the kinetics of the transformations of Ti–20.9 at%V and Ti–21.3 at%V(HP) alloys using differential scanning calorimetry (DSC) measurements (Fig. 2(a)). The peak assignment is based on the previous work [13]. An exothermic peak around 435 K is clearly observed for Ti–21.3 at%V(HP), whereas the corresponding peak can be seen around 500 K for Ti–20.9 at%V. In the peak temperature range measured here, it is shown from the diffusion coefficients [14] that atomic diffusion of Ti and V can hardly influence the phase formation at the given timescale [15]. Therefore, these exothermic peaks are assigned to the DI-ω transformation. It is interesting to note that the peak due to the DI-ω transformation of Ti–21.3 at%V(HP) is shifted to lower temperatures and the absolute quantity of exothermic heat is larger than that of Ti–20.9 at%V. In contrast, the isothermal ω transformation starts only above 550 K, and the peak (arising from isothermal ω) of Ti–21.3 at%V(HP) is found to be smaller than that of Ti–20.9 at%V. This indicates that the total amount of ω transformation (of whichever kind) seems to be approximately constant for the different purities. Upon further heating, inverse transformation from ω to β takes place at around 700 K, and subsequently at higher temperatures α phase is formed in Ti–20.9 at%V, while it is not formed in Ti–21.3 at%V(HP), which suggests that the α phase is induced and stabilized by oxygen. Of course, this phenomenon depends on the heating rate, and the present scan rate of 10 K/min is too fast for the α phase formation in Ti–21.3 at%V(HP). The DSC measurements were repeated twice or more to confirm reproducibility for each of the alloys.

Based on the fact that the DI-ω transformation can take place at 373 K,[15] after the solid-solution treatment, the samples were annealed at 373 K in air for various periods of time to investigate

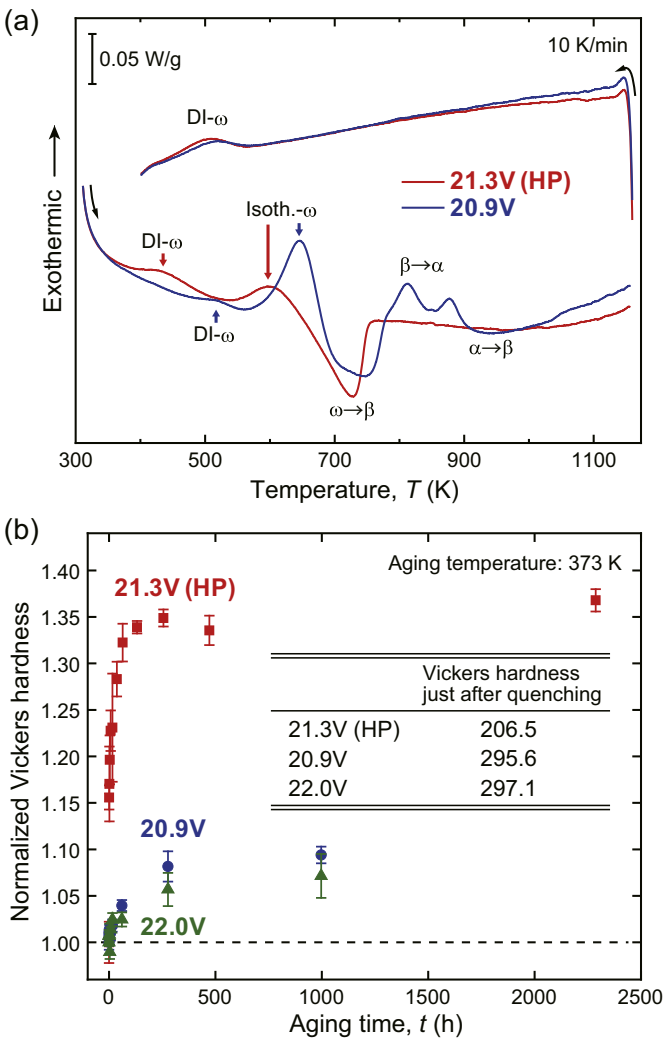

Fig. 2. (a) DSC profiles measured for Ti–20.9 at%V and Ti–21.3 at%V(HP) alloys. The heating/cooling rate was set to 10 K/min. (b) Change in Vickers hardness as a function of annealing time at 373 K. The Vickers hardness is normalized by that of the as-quenched sample.

the effects of oxygen on the hardness changes; the hardness values were measured by using a Vickers hardness (VH) apparatus (Shimadzu HMV-G21). Fig. 2(b) shows the aging time dependence of the Vickers hardness normalized by the Vickers hardness measured immediately after the solid-solution treatment; the initial Vickers hardness values are shown in the table inset in Fig. 2(b). Absolute values of Vickers hardness of Ti–20.9 at%V and Ti–22.0 at%V are significantly higher than those of Ti–21.3 at%V(HP), which means that the hardness is affected by the oxygen content, that is, the solid solution hardening effect clearly appears. Furthermore, it deserves to note that a steep increase in hardness of about 35% is observed within 500 h of aging for Ti–21.3 at%V(HP), whereas the increases for Ti–20.9 at%V and Ti–22.0 at%V are limited to about 10%. This indicates that solute oxygen has a retarding effect on the DI-ω transformation process. This effect is well consistent with the common sense that the oxygen tends to suppress the athermal and isothermal ω transformations.

In a next step, we have investigated the effects of solute oxygen on the resonance frequency f_r and corresponding low-temperature internal friction Q^{-1} for Ti–20.9 at%V, Ti–22.0 at%V and Ti–21.3 at%V(HP) alloys, which were measured with the free-decay method by using electromagnetic acoustic resonance (EMAR) measurements [16]. In the EMAR measurements, quenched cylindrical

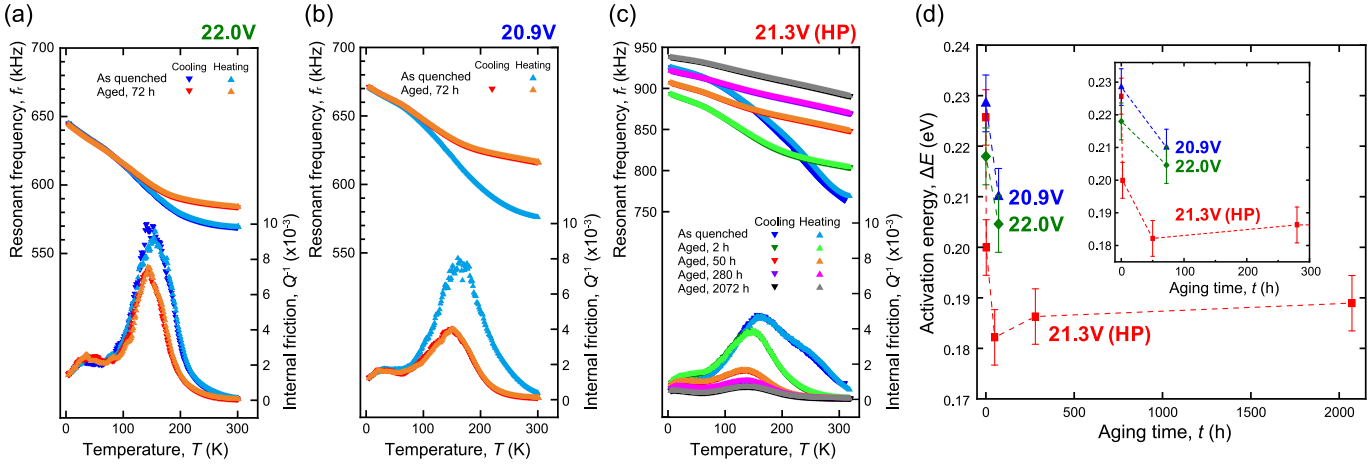

Fig. 3. Resonant frequency f_r and internal friction Q^{-1} as a function of temperature in the submegahertz frequency range obtained for (a) Ti–22.0 at%V, (b) Ti–20.9 at%V, (c) Ti–21.3 at%V(HP), this order corresponds to the temperature value of the peak T_ω: T_ω(22.0V) < T_ω(20.9V) < T_ω(21.3V-HP). (d) The activation energy $\Delta E_{\{111\}}$ as a function of aging time at 373 K. The inset shows a magnification of the early stage of aging.

samples were cooled down from 300 to 4 K. In addition to the quenched state, the same measurement was conducted after annealing at 373 K for 72 h for the Ti–20.9 at%V and Ti–22.0 at%V alloys and after 2, 50, 280 and 2072 h for the Ti–21.3 at%V(HP) alloy. All the measurement parameters were kept constant in all the experiments.

Previous works [11,15,17–19], substantiated that the low-temperature internal friction in the submegahertz frequency range represents the elementary process, i.e., the dynamic $\{111\}_\beta$ collapse which is considered to be the core reason for the ω transformation. Fig. 3(a–c) shows the changes in the resonance frequency f_r and internal friction Q^{-1} during the cooling processes in the Ti–22.0 at%V, Ti–20.9 at%V, Ti–21.3 at%V(HP) alloys after quenching from 1073 K and after subsequent aging at 373 K for 72 h. Although the resonance frequency f_r increases with a decrease in temperature below 300 K for all the alloys, an inflexion (ΔM effect due to the dynamic $\{111\}_\beta$ collapse) can be clearly observed at around 180 K. What should be noted here is that the change in Q^{-1} depends on the value of the athermal ω transformation temperature: T_ω(22.0V) < T_ω(20.9V) < T_ω(21.3V-HP). It is found that the higher T_ω is, the more rapidly the DI-ω transformation proceeds. Furthermore, although the content of the β-stabilizer (vanadium) in Ti–21.3 at%V(HP) is higher than that of Ti–20.9 at%V, the DI-ω transformation is more pronounced in Ti–21.3 at%V(HP) compared to Ti–20.9 at%V. Notably, after aging for only 50 h at 373 K, the height of Q^{-1} drastically reduces down to about 20% of the initial value for Ti–21.3 at%V(HP), whereas that for Ti–20.9 at%V drops only to about 50% even after aging for a longer time, namely 72 h, at the same temperature. It can thus be concluded that the solute oxygen atoms are also effective in suppressing the DI-ω transformation.

By using a Debye type damping function to analyze the $Q^{-1}(T)$ profiles measured for these alloys,

$$Q^{-1} = \Delta \frac{\omega_r \tau}{1 + (\omega_r \tau)^2}, \qquad \tau = \tau_0 \exp\left(\frac{\Delta E_{\{111\}}}{kT}\right), \tag{1}$$

we derive the activation energies $\Delta E_{\{111\}}$ of the dynamic $\{111\}_\beta$ collapse, where Δ is the relaxation strength, $\omega_r (= 2\pi f_r)$ the angular frequency, and τ_0 the time constant; according to literature,[17] $\tau_0 = 2.2 \times 10^{-14}$ s. Since the measured, broad $Q^{-1}(T)$ profiles cannot be correctly reproduced by the Debye function as indicated by our previous paper [11], we approximately deduce the activation energies $\Delta E_{\{111\}}$ by using only the relation between peak temperature and frequency. Under the condition that $\omega_r \tau = 1$ holds at the peak position, we have

$$\Delta E_{\{111\}} = -kT_p \ln(\omega_r \tau_0). \tag{2}$$

Fig. 3(d) shows the aging-time dependence of the activation energy $\Delta E_{\{111\}}$ for Ti–20.9 at%V, Ti–22.0 at%V, and Ti–21.3 at%V(HP). The activation energies of the $\{111\}_\beta$ collapse are found to be in the range of 0.18-0.23 eV, being consistent with previous values [11,17]. Interestingly, for all the alloys, the values of $\Delta E_{\{111\}}$ steeply decrease with aging time, thus, with the progress of the DI-ω transformation, which is qualitatively very similar to the aging-time dependence of the Vickers hardness in Fig. 2(b). The decrease in $\Delta E_{\{111\}}$ with aging time implies that the local regions of the β matrix which have larger activation energies tend to be annihilated more preferentially with aging. Currently, there is no approach to rationalize this somewhat intriguing feature, but the activation energy of about 0.2 eV is not a rate-controlling factor around RT or 373 K, so it may well be that other variables beside the magnitude of $\Delta E_{\{111\}}$ also contribute to the observed phenomenon.

Finally, we have investigated whether the ω phase formation in Ti–21.3 at%V(HP) progresses more rapidly than the formation in Ti–20.9 at%V and Ti–22.0 at%V. Fig. 4 shows the X-ray diffraction (XRD) profiles obtained for those samples aged at RT for more than one week. It is clearly seen that the diffraction peak corre-

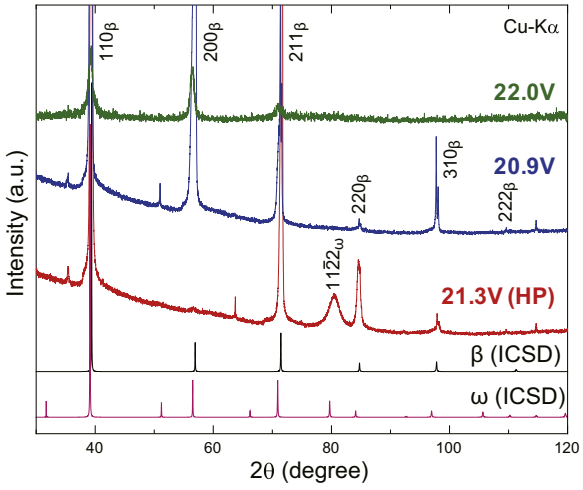

Fig. 4. XRD profiles obtained for Ti–20.9 at%V, Ti–22.0 at%V, and Ti–21.3 at%V(HP), which were subjected to room temperature aging for more than one week.

sponding to the ω phase exists in the XRD profile obtained for Ti–21.3 at%V(HP). Thus, the rapid changes in the Vickers hardness and internal-friction intensity observed for Ti–21.3 at%V(HP) is attributed to the fact that the DI-ω mode is significantly facilitated in case of fewer solute oxygen atoms.

In conclusion, we have revealed the oxygen effects on the DI-ω transformation with a special focus on the changes in Vickers hardness, and internal friction upon aging. The latter method was used to assess the dynamic $\{111\}_\beta$ collapse in the ω transformation. Salient results can be drawn as follows.

1. Solute oxygen atoms tend to suppress the DI-ω transformation above T_ω. This characteristic feature is not contradictive to the general knowledge that has been well established for β-Ti alloys.
2. The β-Ti–V alloy with fewer solute oxygen atoms undergoes a very rapid DI-ω transformation. Accompanied with this, the Vickers hardness steeply increases with aging time at low temperatures above T_ω, where the atomic diffusion is sufficiently suppressed. On the other hand, despite the similar V content, the alloys with a solute oxygen concentration of about 1% undergo the DI-ω transformation retardedly.
3. The internal friction peak is drastically attenuated as the DI-ω transformation proceeds with aging. Furthermore, also the activation energy decreases with aging. It is interesting to note that the regions with larger activation energies for the dynamic $\{111\}_\beta$ collapse are preferentially annihilated during the progress of the DI-ω transformation in the low-temperature aging experiments.

Declaration of Competing Interest

The authors declare that they have no known competing financial interests or personal relationships that could have appeared to influence the work reported in this paper.

Acknowledgments

This work was supported by JST, PRESTO Grant Number JPMJPR1996, and JSPS KAKENHI Grant No. 19H04408, Japan. The authors acknowledge the staffs of Analytical Research Core for Advanced Materials (ARCAM), Institute for Materials Research of Tohoku University.

References

[1] P.D. Frost, W.M. Parris, L.L. Hirsch, J.R. Doig, C.M. Schwartz, Trans. Am. Soc. Metals 46 (1954) 231–256.
[2] B.S. Hickman, J. Mater. Sci. 4 (1969) 554–563.
[3] D. de Fontaine, N.E. Paton, J.C. Williams, Acta Metall. 19 (1971) 1153–1162.
[4] S.K. Sikka, Y.K. Vohra, R. Chidambaram, Prog. Mater. Sci. 27 (1982) 245–310.
[5] S. Nag, A. Devaraj, R. Srinivasan, R.E.A. Williams, N. Gupta, G.B. Viswanathan, J.S. Tiley, S. Banerjee, S.G. Srinivasan, H.L. Fraser, R. Banerjee, Phys. Rev. Lett. 106 (2011) 245701.
[6] M.J. Lai, C.C. Tasan, J. Zhang, B. Grabowski, L.F. Huang, D. Raabe, Acta Mater. 92 (2015) 55–63.
[7] D. Choudhuri, Y. Zheng, T. Alam, R. Shi, M. Hendrickson, S. Banerjee, Y. Wang, S.G. Srinivasan, H. Fraser, R. Banerjee, Acta Mater. 130 (2017) 215–228.
[8] C.B. Walker, Phys. Rev. B 28 (1983) 674–688.
[9] Z. Fan, Scr. Metall. Mater. 31 (1994) 1519–1524.
[10] Y. Al-Zain, Y. Sato, H.Y. Kim, H. Hosoda, T.H. Nam, S. Miyazaki, Acta Mater. 60 (2012) 2437–2447.
[11] M. Tane, H. Nishiyama, A. Umeda, N.L. Okamoto, K. Inoue, M. Luckabauer, Y. Nagai, T. Sekino, T. Nakano, T. Ichitsubo, Phys. Rev. Mater. 3 (2019) 043604.
[12] N.E. Paton, J.C. Williams, Scr. Metall. 7 (1973) 647–649.
[13] M. Bönisch, A. Panigrahi, M. Stoica, M. Calin, E. Ahrens, M. Zehetbauer, W. Skrotzki, J. Eckert, Nat. Commun. 8 (2017) 1429.
[14] J.F. Murdock, C.J. Mchargue, Acta Metall. 16 (1968) 493–509.
[15] N.L. Okamoto, S. Kasatani, M. Luckabauer, R. Enzinger, S. Tsutsui, M. Tane, T. Ichitsubo, Acta Mater. (2020) (Submitted).
[16] M. Hirao, H. Ogi, EMATs for Science and Industry: Noncontacting Ultrasonic Measurements, Kluwer Academic Publishers, Dordrecht, 2013.
[17] A.W. Sommer, S. Motokura, K. Ono, O. Buck, Acta Metall. 21 (1973) 489–497.
[18] C.W. Nelson, D.F. Gibbons, R.F. Hehemann, J. Appl. Phys. 37 (1966) 4677–4682.
[19] J.E. Doherty, D.F. Gibbons, Acta Metall. 19 (1971) 275–282.